A Helical Peptide can Mediate Electron over 120 Å by Hopping Mechanism

T. Morita, Y. Arikuma, H. Nakayama, and S. Kimura

Department of Material Chemistry, Graduate School of Engineering, Kyoto University
Room A3-204, Kyoto-Daigaku-Katsura, Nishikyo-ku, Kyoto 615-8510, Japan,
morita@peptide.polym.kyoto-u.ac.jp, arikuma@peptide.polym.kyoto-u.ac.jp,
nakayama@peptide.polym.kyoto-u.ac.jp, shun@scl.kyoto-u.ac.jp

ABSTRACT

α-Helices in natural proteins are considered to play important roles in long-range electron transfer, but the details are yet to be clarified. We have prepared well-defined self-assembled monolayers on gold of helical peptides of different lengths from 8mer to 80mer, and studied the electron transfer through the helices electrochemically. We have observed non-exponential distance dependence and high activation energies of the electron transfer, suggesting a hopping mechanism with the amide groups as hopping sites, which have been successfully validated by in-depth theoretical calculations. Importantly, an electron is transferred at rate constants of 0.1-10 s^{-1} across the 80mer helical peptide monolayer and the electron-transfer distance is over 120 Å assuming intramolecular electron transfer along the helix.

Keywords: helical peptide, ferrocene, self-assembled monolayer, electron transfer, hopping mechanism

1 INTRODUCTION

Long-range electron transfer has been of a great interest from viewpoints of clarification of biological electron-transfer phenomena and realization of molecular electronics. One of the most interesting points of the biological electron transfer is long-range electron-transfer reactions in proteins which cannot be explained by the conventional electron-tunneling theories directly from donor to acceptor. To answer this question, we have studied distance dependence of the electron transfer through helical peptide self-assembled monolayers prepared on a gold surface [1,2]. Various lengths of helical peptides, 8mer, 16mer, 32mer, 48mer, 64mer, and 80mer carrying a redox-active ferrocene unit and a disulfide group at the respective terminals (Figure 1) were synthesized by liquid-phase methods. The helix part is of an alternating sequence of L-alanine and α-aminoisobutyric acid, which has been shown to take stable α-helical conformation. Each peptide was immobilized on gold via a gold-sulfur linkage to form a self-assembled monolayer. The helical peptides formed a well-packed monolayer with homogeneous molecular orientation, revealed by ellipsometry, infrared spectroscopy, and cyclic voltammetry, along with theoretical calculations. The electron transfer from the ferrocene unit to gold through the helical peptides was studied by electrochemistry. Cyclic voltammetry showed reversible redox peaks of the ferrocene moiety, indicating that the electron transfer occurs between the ferrocene moiety and gold through the helical peptide monolayer. The standard electron-transfer rate constants were determined by electron chemical impedance spectroscopy. The rate constants showed a very shallow distance dependence of the electron transfer rates and high activation energies, both of which are characteristic of a hopping mechanism. Detailed theoretical calculations taking into account electrostatic potential profile and image dipole-stabilization energies have successfully demonstrated that a hopping mechanism with the amide groups as hopping sites is responsible for the long-range electron transfer. Furthermore, for the 80mer helical peptide, we observed a unique dependence of the electron transfer on the monolayer packing, suggesting the importance of structural fluctuations of the peptides on the electron transfer which is governed by the hopping mechanism. This work has implications for biological electron transfer and molecular-based electronics. Contributions of hopping among side chains of aromatic amino acids in electron transfer through model helical peptides and long-range electron transfer in proteins have been demonstrated. In contrast, this work suggests that the intrinsic peptide backbone can also serve as stepping stones. Hopping among amide groups might be involved in some long-range electron transfer if oxidation or reduction of the amide groups is energetically available. Studies on electron transfer reactions in the relations with peptide secondary structures are thus essential for understanding important electron-transport phenomena in protein systems such as photosynthesis, respiration, enzymatic catalysis, damage transfer, and so on. Not only that, peptide secondary structures have attracted much attention as promising candidates for components in molecular electronics because of their great latitude in chemical design, well-defined structures and superior self-assembling properties, and unique electric features. For example, ferrocene-terminated helical peptide monolayers can be used as unique interfaces between electron-transfer proteins and gold, in which the proteins can be immobilized retaining their natural structure and long-range electron communication between gold, ferrocene, and redox groups in the proteins is ensured. Such hybrid molecular systems sound promising for efficient solar-energy conversion, artificial catalysis, and biosensing.

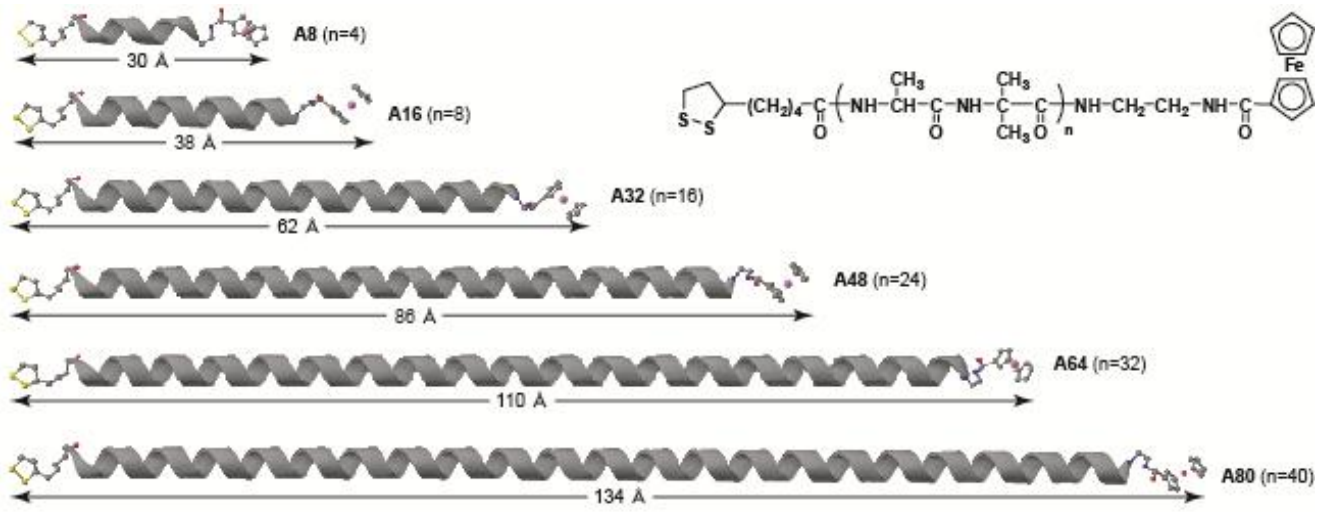

Figure 1: Chemical structures and schematic illustrations of the helical peptides used in this study.

2 EXPERIMENTAL

2.1 Synthesis and Spectroscopy in Solution

The helical peptides were synthesized by the liquid-phase method. All the intermediates were identified by ^{1}H-NMR spectroscopy and the final products were further confirmed by MALDI-TOF mass spectrometry. The purity of the intermediates was checked by thin-layer chromatography and the purity of the final compound was checked by high performance liquid chromatography. Circular dichroism (CD) spectra of the helical peptides in trifluoroethanol were measured on a CD spectropolarimeter at a residue concentration of 1.8×10^{-3} M with an optical cell of 0.1 cm optical path length at room temperature.

2.2 Monolayer Preparation

A glass slide was cleaned by sulfuric acid, rinsed with water and methanol, and dried in vacuum. A gold substrate was prepared by vapor deposition of chromium (300 Å) and then gold (99.99 %, 2000 Å) onto the glass slide by a vacuum deposition system. The prepared gold substrate was immediately used for self-assembling. The peptide was dissolved in appropriate organic solvent (ca. 0.1 mM) and a gold substrate was immersed in the solution for 24 h. After immersion, the substrate was thoroughly rinsed with appropriate organic solvent, and dried with a N_2 stream and in vacuum for 15 min.

2.3 Monolayer Characterizations

Infrared reflection-absorption spectroscopy (IRRAS) were performed on a Fourier transform infrared spectrometer at room temperature in dry air with a reflection attachment. The incident angle was set at 84º from the surface normal. The number of interferogram accumulations was 200. The tilt angles of the helix axis from the surface normal was determined on the basis of the amide I/II absorbance ratios by comparing the experimental spectra with theoretically-simulated spectra. Ellipsometry was carried out by an auto-ellipsometer at room temperature to determine the monolayer thicknesses. A helium-neon laser with a wavelength of 632.8 nm was used as the incident light at an incident angle of 65º. The complex optical constant of the monolayers was assumed to be 1.50+0.00i. For each monolayer sample, the thicknesses were measured on more than 5 different spots on the surface and the data were averaged.

2.4 Electrochemical Measurements

Electrochemical experiments were performed by voltammetric analyzers for cyclic voltammetry (CV), and a combination of impedance/gain-phase analyzer and electrochemical interface for electrochemical impedance spectroscopy (EIS). A three-electrode system was used with the monolayer-modified gold substrate as the working electrode, Ag/AgCl in a 3 M NaCl aqueous solution as the reference electrode, and a platinum wire as the auxiliary electrode. The solution was a 1 M $HClO_4$ aqueous solution. The solution was deaerated with N_2 gas for 15 min prior to the experiments. The area of the working electrode exposed to the electrolyte solution was 0.9−1.1 cm^2. CV was performed at various scan rates of 0.1−0.5 V/s. The surface densities of the ferrocene unit were calculated by integration of the anodic peaks after subtraction of the background current. EIS was performed at the formal oxidation potential of the ferrocene unit (0.45 V) with a DC voltage of 10 mV at frequencies from 10^5 Hz to the

frequency lower than the time constant of the electron transfer (10^{-3}–10^{-1} Hz). The obtained results in the form of the Bode plot were fitted by an equivalent circuit consisting of solution resistance (R_s), monolayer constant-phase element (CPE, $Z_{CPE}=(1/(Q(i\omega)^n))$), and electron-transfer resistance (R_{et}) and capacitance (C_{et}). In this study, a CPE was used instead of a simple capacitance to get better agreement between the experimental and simulated curves by accounting for inhomogeneity of the electrode surface. The standard electron-transfer rate constants (k_{et}^0s) were calculated by $k_{et}^0=1/(2R_{et}C_{et})$. For temperature-variable measurements to determine the activation energies, EIS was performed with a home-made copper vessel which accommodated the electrochemical cell and was connected to a temperature-controlled bath. The k_{et}^0 values at four different temperatures were analyzed by the Arrhenius plot to afford the activation energies.

2.5 Theoretical Calculations

Molecular lengths and cross-sectional areas were estimated on the basis of computational geometry optimization for the respective helical peptides. The theoretical monolayer thicknesses were approximated by (molecular length)×cos(tilt angle from IRRAS). The theoretical peptide surface densities were estimated from the cross-sectional area of the helix and the tilt angles. Assuming hexagonal packing with a tilt angle of 0^o, the limiting surface densities were calculated, and the theoretical surface densities were estimated by (limiting surface density)×cos(tilt angle from IRRAS). The standard electron-transfer rate constants were theoretically calculated for electron tunneling and a hopping mechanism with the amide groups as hopping sites.

3 RESULTS AND DISCUSSION

A8, A16, A32, A48, A64, and A80 were successfully synthesized. CD spectroscopy in solution showed that A8 takes 3_{10}-helical conformation while the rest of the peptides take α-helical conformation, which agrees with the previous studies using similar peptides.

Each peptide was immobilized on a gold surface via a gold-sulfur linkage to form a self-assembled monolayer by immersion of a gold substrate into the peptide solution. First, molecular orientation was examined by IRRAS. Amide I and II bands were observed at 1680−1670 cm^{-1} and around 1540 cm^{-1}, respectively. The tilt angles of the helices from the surface normal are summarized in Table 1. The tilt angles show that the helices become more vertical as the chain is elongated up to 64mer. This finding can be explained by stronger intermolecular interactions among the longer helices, resulting in more vertical orientation. On the other hand, the tilt angle of A80 is larger than that of A64. The poor solubility of A80 into the preparation solution might have led to formation of a loosely-packed monolayer. Up to 64mer, the experimental results of the monolayer thicknesses and the surface densities are well consistent with the calculated results on the basis of the tilt angles (Table 1), indicating that the peptides form a well-packed monolayer with homogeneous orientation. Blocking experiments in a ferrocyanide solution confirmed the well-packed property of the monolayers besides the A80 monolayer.

Table 1: Summary of this work.

peptide	A8	A16	A32	A48	A64	A80
tilt angle (degree)	49.4	43.7	35.0	26.2	23.1	37.2
calculated monolayer thickness (Å)	10.4	17.4	39.3	64.6	88.3	94.8
experimental monolayer thickness (Å)	11.7	24.9	38.4	50.9	77.1	74.9
calculated surface density ($\times10^{-11}$ mol/cm^2)	14.0	11.9	13.5	14.8	15.2	13.0
experimental surface density ($\times10^{-11}$ mol/cm^2)	17.3	15.1	13.5	11.1	10.2	3.3
experimental k_{et}^0 (s^{-1})	1725	71.5	5.43	1.28	0.45	2.6
calculated k_{et}^0 for hopping mechanism (s^{-1})	887	195	11.4	1.77	0.58	0.38
calculated k_{et}^0 for tunneling mechanism (s^{-1})	12.0	0.10	5.5×10^{-8}	3.1×10^{-14}	1.7×10^{-20}	1.0×10^{-26}
experimental activation energy (eV)	0.42	0.40	0.36	0.45	0.51	0.57
calculated activation energy (eV)	0.38	0.42	0.50	0.55	0.57	0.58

To study the electron transfer from the ferrocene unit to gold, CV was carried out in a $HClO_4$ aqueous solution. In all the SAMs, reversible redox peaks of ferrocenium/ferrocene are clearly observed, surprisingly even in the A80 SAM, showing that an electron is exchanged between the ferrocene unit and gold. The formal potentials are ca. 0.45 V in all the SAMs. Next, EIS was performed to determine the k_{et}^0s (Table 1). Figure 2 shows the semilog plot of k_{et}^0s over the ellipsometry thicknesses. The nonlinear relationship in the semilog plot clearly indicates that the electron transfer through these helices is not governed by the conventional electron tunneling which should show a linear relationship with a slope of the decay constant. For reference, a linear distance dependence of electron tunneling is also shown as a dotted line in Figure 2, which is too steep to explain the present data, suggesting a hopping mechanism. The activation energies were determined by variable-temperature measurements (Table 1). If electron tunneling is operative, the activation energy is ca. 0.2 eV which is one-fourth of the reported reorganization energy of a ferrocene moiety. The observed activation energies significantly larger than 0.2 eV also suggests contribution of a hopping mechanism. The plausible hopping sites are the amide groups and it is likely that a hole hops among the amide groups with taking the frontier orbital levels of an amide group into consideration, that is, the HOMO of the amide is close to the Fermi level. Therefore, an electron is first transferred from the N-terminal amide group to gold to generate the cation radical of the amide group, the cation radical hops among the amide group to reach the C-terminal, and finally it is

reduced by the ferrocene unit, completing the overall electron transfer from the ferrocene unit to gold.

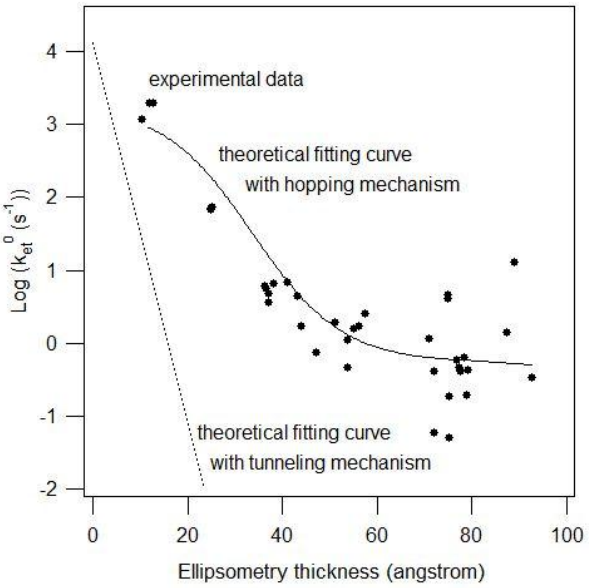

Figure 2: Distance dependece of the standard electron-transfer rate constants for the helical peptides.

To quantitatively discuss the results, theoretical calculations of k_{et}^0s were carried out. k_{et}^0 is the sum of the rate constants of the electron tunneling and the hopping mechanism. The rate constants of electron tunneling were calculated by a formalism for interfacial molecule-metal electron transfer. On the other hand, the rate constants for the hopping mechanism were determined as follows. First, the electrostatic-potential profiles in the monolayer and the stabilization energies of the amide cation radicals due to the image dipole formed inside the metal were calculated. The oxidation potential of an amide group in a peptide chain was determined by CV in DMF. The oxidation potential was determined to be 0.93 V vs. Ag/AgCl. From this oxidation potential along with the electrostatic potential and image-dipole stabilization energies, the amide oxidation potentials in the monolayers were determined. The dipole moment of the helix was taken into account by locating partial charges at the terminals. From these oxidation potentials, the rate constants of the respective electron-tunneling steps were calculated by formalisms for inhomogeneous molecule-metal and homogeneous molecule-molecule electron transfer. The rate constant of the hole transfer among the amide groups was calculated to be on the order of 10^{10} s^{-1}. Finally, using these rate constants, the overall rate constants were calculated by the Ratner's formalism [3].

The calculated k_{et}^0s are summarized in Table 1 and the theoretical curves are shown in Figure 2 as a solid line. The calculations excellently reproduce the experimental k_{et}^0s. It is found that the hopping mechanism is dominant in all the peptides. Previously, we speculated that the electron tunneling was prevailing in the 8mer SAM simply because of the relatively large decay constant. However, the hopping mechanism is found here to be dominant even in the 8mer helical peptide.

The activation energies (Table 1) are also calculated from theoretical k_{et}^0s at 298 K and 323K. They are well consistent with the experimental values, and are significantly larger than that of the tunneling case. Reasonably, the activation energies are found to correspond to the energy gaps between the gold Fermi level and the oxidation potential of the amide group which shows the most positive value in the energy diagram. The good agreements of the theoretical and experimental data conclude that the hopping mechanism is responsible for the long-range electron transfer, and accordingly the electron transfer is persistent over long distances with measurable electron transfer rate constants. Importantly, an electron is transferred at a moderate rate constant in the 80mer helical peptide, and the electron-transfer distance is over 120 Å, assuming the intramolecular electron transfer along the helix.

Molecular-dynamics-associated or conformational-gating electron tunneling has been proposed to explain a shallow distance dependence, in which a peptide chain thermally fluctuates to reach an active conformer enabling efficient electron tunneling. However, it is unlikely that a helix shrinks, bends, or tilts to a large extent to reduce the electron-transfer distance down to an electron-tunneling range in a well-packed monolayer especially of the present long helices with parallel arrangement. Therefore, a simple picture of molecular dynamics with global motions cannot explain our results.

4 CONCLUSIONS

We have systematically studied long-range electron transfer through well-defined monolayers composed of various lengths of helical peptides, and successfully demonstrated that a hopping mechanism with the amide groups as hopping sites is responsible for the long-range electron transfer.

REFERENCES

[1] Y. Arikuma, T. Morita, H, Nakayama, and S Kimura, "Electron Hopping over 100 Å Along an α-Helix", Angew. Chem. Int. Ed., 49, 1800-1804, 2010.

[2] Y. Arikuma, H. Nakayama, T. Morita, and S. Kimura, "Ultra-Long-Range Electron Transfer through a Self-Assembled Monolayer on Gold Composed of 120-Å-Long α-Helices", Langmuir, 27, 1530–1535, 2011.

[3] Y. A. Berlin and M. A. Ratner, "Intra-molecular Electron Transfer and Electric Conductance via Sequential Hopping: Unified Theoretical Description", Radiat. Phys. Chem., 74, 124-131, 2005.